Editors' Suggestion | Featured in Physics

Cosmological Constraints from Multiple Probes in the Dark Energy Survey

T. M. C. Abbott,[1] A. Alarcon,[2,3] S. Allam,[4] P. Andersen,[5,6] F. Andrade-Oliveira,[7,8] J. Annis,[4] J. Asorey,[9] S. Avila,[10] D. Bacon,[10] N. Banik,[4] B. A. Bassett,[11,12] E. Baxter,[13] K. Bechtol,[14,15] M. R. Becker,[16] G. M. Bernstein,[13] E. Bertin,[17,18] J. Blazek,[19,20] S. L. Bridle,[21] D. Brooks,[22] D. Brout,[13] D. L. Burke,[23,24] J. Calcino,[5] H. Camacho,[25,8] A. Campos,[26,7] A. Carnero Rosell,[27,8] D. Carollo,[28] M. Carrasco Kind,[29,30] J. Carretero,[31] F. J. Castander,[2,3] R. Cawthon,[15] P. Challis,[32] K. C. Chan,[2,3] C. Chang,[33,34] M. Childress,[35] M. Crocce,[2,3] C. E. Cunha,[23] C. B. D'Andrea,[13] L. N. da Costa,[8,36] C. Davis,[23] T. M. Davis,[5] J. De Vicente,[27] D. L. DePoy,[37] J. DeRose,[38,23] S. Desai,[39] H. T. Diehl,[4] J. P. Dietrich,[40,41] S. Dodelson,[26] P. Doel,[22] A. Drlica-Wagner,[4,34] T. F. Eifler,[42,43] J. Elvin-Poole,[19,44] J. Estrada,[4] A. E. Evrard,[45,46] E. Fernandez,[31] B. Flaugher,[4] R. J. Foley,[47] P. Fosalba,[2,3] J. Frieman,[4,34] L. Galbany,[48] J. García-Bellido,[49] M. Gatti,[31] E. Gaztanaga,[2,3] D. W. Gerdes,[45,46] T. Giannantonio,[50,51,52] K. Glazebrook,[53] D. A. Goldstein,[54] D. Gruen,[38,23,24] R. A. Gruendl,[29,30] J. Gschwend,[8,36] G. Gutierrez,[4] W. G. Hartley,[22,55] S. R. Hinton,[5] D. L. Hollowood,[47] K. Honscheid,[19,44] J. K. Hoormann,[5] B. Hoyle,[56,52] D. Huterer,[46] B. Jain,[13] D. J. James,[57] M. Jarvis,[13] T. Jeltema,[47] E. Kasai,[58,12] S. Kent,[4,34] R. Kessler,[33,34] A. G. Kim,[59] N. Kokron,[38,23] E. Krause,[42] R. Kron,[4,34] K. Kuehn,[60] N. Kuropatkin,[4] O. Lahav,[22] J. Lasker,[33,34] P. Lemos,[22,50,51] G. F. Lewis,[61] T. S. Li,[4,34] C. Lidman,[62] M. Lima,[25,8] H. Lin,[4] E. Macaulay,[10] N. MacCrann,[19,44] M. A. G. Maia,[8,36] M. March,[13] J. Marriner,[4] J. L. Marshall,[37] P. Martini,[19,63] R. G. McMahon,[50,51] P. Melchior,[64] F. Menanteau,[29,30] R. Miquel,[65,31] J. J. Mohr,[40,41,56] E. Morganson,[30] J. Muir,[23] A. Möller,[66,62] E. Neilsen,[4] R. C. Nichol,[10] B. Nord,[4] R. L. C. Ogando,[8,36] A. Palmese,[4] Y. -C. Pan,[67,68] H. V. Peiris,[22] W. J. Percival,[69,70] A. A. Plazas,[64] A. Porredon,[2,3] J. Prat,[31] A. K. Romer,[71] A. Roodman,[23,24] R. Rosenfeld,[72,8] A. J. Ross,[19] E. S. Rykoff,[23,24] S. Samuroff,[26] C. Sánchez,[13] E. Sanchez,[27] V. Scarpine,[4] R. Schindler,[24] M. Schubnell,[46] D. Scolnic,[76] L. F. Secco,[13] S. Serrano,[2,3] I. Sevilla-Noarbe,[27] R. Sharp,[62] E. Sheldon,[73] M. Smith,[35] M. Soares-Santos,[74] F. Sobreira,[75,8] N. E. Sommer,[66,62] E. Swann,[10] M. E. C. Swanson,[30] G. Tarle,[46] D. Thomas,[10] R. C. Thomas,[59] M. A. Troxel,[76] B. E. Tucker,[66,62] S. A. Uddin,[77] P. Vielzeuf,[31] A. R. Walker,[1] M. Wang,[4] N. Weaverdyck,[46] R. H. Wechsler,[38,23,24] J. Weller,[40,56,52] B. Yanny,[4] B. Zhang,[66,62] Y. Zhang,[4] and J. Zuntz[78]

(DES Collaboration)

[1]*Cerro Tololo Inter-American Observatory, National Optical Astronomy Observatory, Casilla 603, La Serena, Chile*
[2]*Institut d'Estudis Espacials de Catalunya (IEEC), 08034 Barcelona, Spain*
[3]*Institute of Space Sciences (ICE, CSIC), Campus UAB, Carrer de Can Magrans, s/n, 08193 Barcelona, Spain*
[4]*Fermi National Accelerator Laboratory, P. O. Box 500, Batavia, Illinois 60510, USA*
[5]*School of Mathematics and Physics, University of Queensland, Brisbane, QLD 4072, Australia*
[6]*University of Copenhagen, Dark Cosmology Centre, Juliane Maries Vej 30, 2100 Copenhagen O, Denmark*
[7]*Instituto de Física Teórica, Universidade Estadual Paulista, São Paulo, Brazil*
[8]*Laboratório Interinstitucional de e-Astronomia—LIneA, Rua Gal. José Cristino 77, Rio de Janeiro, RJ 20921-400, Brazil*
[9]*Korea Astronomy and Space Science Institute, Yuseong-gu, Daejeon 305-348, Korea*
[10]*Institute of Cosmology and Gravitation, University of Portsmouth, Portsmouth PO1 3FX, United Kingdom*
[11]*African Institute for Mathematical Sciences, 6 Melrose Road, Muizenberg 7945, South Africa*
[12]*South African Astronomical Observatory, P.O.Box 9, Observatory 7935, South Africa*
[13]*Department of Physics and Astronomy, University of Pennsylvania, Philadelphia, Pennsylvania 19104, USA*
[14]*LSST, 933 North Cherry Avenue, Tucson, Arizona 85721, USA*
[15]*Physics Department, 2320 Chamberlin Hall, University of Wisconsin-Madison, 1150 University Avenue Madison, Wisconsin 53706-1390, USA*
[16]*Argonne National Laboratory, 9700 South Cass Avenue, Lemont, Illinois 60439, USA*
[17]*CNRS, UMR 7095, Institut d'Astrophysique de Paris, F-75014 Paris, France*
[18]*Sorbonne Universités, UPMC Univ Paris 06, UMR 7095, Institut d'Astrophysique de Paris, F-75014 Paris, France*
[19]*Center for Cosmology and Astro-Particle Physics, The Ohio State University, Columbus, Ohio 43210, USA*
[20]*Institute of Physics, Laboratory of Astrophysics, École Polytechnique Fédérale de Lausanne (EPFL), Observatoire de Sauverny, 1290 Versoix, Switzerland*
[21]*Jodrell Bank Center for Astrophysics, School of Physics and Astronomy, University of Manchester, Oxford Road, Manchester, M13 9PL, United Kingdom*
[22]*Department of Physics & Astronomy, University College London, Gower Street, London WC1E 6BT, United Kingdom*
[23]*Kavli Institute for Particle Astrophysics & Cosmology, P. O. Box 2450, Stanford University, Stanford, California 94305, USA*
[24]*SLAC National Accelerator Laboratory, Menlo Park, California 94025, USA*

[25]Departamento de Física Matemática, Instituto de Física, Universidade de São Paulo, CP 66318, São Paulo, SP 05314-970, Brazil
[26]Department of Physics, Carnegie Mellon University, Pittsburgh, Pennsylvania 15312, USA
[27]Centro de Investigaciones Energéticas, Medioambientales y Tecnológicas (CIEMAT), Madrid, Spain
[28]INAF, Astrophysical Observatory of Turin, I-10025 Pino Torinese, Italy
[29]Department of Astronomy, University of Illinois at Urbana-Champaign, 1002 W. Green Street, Urbana, Illinois 61801, USA
[30]National Center for Supercomputing Applications, 1205 West Clark St., Urbana, Illinois 61801, USA
[31]Institut de Física d'Altes Energies (IFAE), The Barcelona Institute of Science and Technology, Campus UAB, 08193 Bellaterra (Barcelona) Spain
[32]Harvard-Smithsonian Center for Astrophysics, 60 Garden St., Cambridge, Massachusetts 02138, USA
[33]Department of Astronomy and Astrophysics, University of Chicago, Chicago, Illinois 60637, USA
[34]Kavli Institute for Cosmological Physics, University of Chicago, Chicago, Illinois 60637, USA
[35]School of Physics and Astronomy, University of Southampton, Southampton SO17 1BJ, United Kingdom
[36]Observatório Nacional, Rua Gal. José Cristino 77, Rio de Janeiro, RJ 20921-400, Brazil
[37]George P. and Cynthia Woods Mitchell Institute for Fundamental Physics and Astronomy, and Department of Physics and Astronomy, Texas A&M University, College Station, Texas 77843, USA
[38]Department of Physics, Stanford University, 382 Via Pueblo Mall, Stanford, California 94305, USA
[39]Department of Physics, IIT Hyderabad, Kandi, Telangana 502285, India
[40]Excellence Cluster Universe, Boltzmannstr. 2, 85748 Garching, Germany
[41]Faculty of Physics, Ludwig-Maximilians-Universität, Scheinerstr. 1, 81679 Munich, Germany
[42]Department of Astronomy/Steward Observatory, 933 North Cherry Avenue, Tucson, Arizona 85721-0065, USA
[43]Jet Propulsion Laboratory, California Institute of Technology, 4800 Oak Grove Dr., Pasadena, California 91109, USA
[44]Department of Physics, The Ohio State University, Columbus, Ohio 43210, USA
[45]Department of Astronomy, University of Michigan, Ann Arbor, Michigan 48109, USA
[46]Department of Physics, University of Michigan, Ann Arbor, Michigan 48109, USA
[47]Santa Cruz Institute for Particle Physics, Santa Cruz, California 95064, USA
[48]PITT PACC, Department of Physics and Astronomy, University of Pittsburgh, Pittsburgh, Pennsylvania 15260, USA
[49]Instituto de Fisica Teorica UAM/CSIC, Universidad Autonoma de Madrid, 28049 Madrid, Spain
[50]Institute of Astronomy, University of Cambridge, Madingley Road, Cambridge CB3 0HA, United Kingdom
[51]Kavli Institute for Cosmology, University of Cambridge, Madingley Road, Cambridge CB3 0HA, United Kindom
[52]Universitäts-Sternwarte, Fakultät für Physik, Ludwig-Maximilians Universität München, Scheinerstr. 1, 81679 München, Germany
[53]Centre for Astrophysics & Supercomputing, Swinburne University of Technology, VIC 3122, Australia
[54]California Institute of Technology, 1200 East California Blvd, MC 249-17, Pasadena, California 91125, USA
[55]Department of Physics, ETH Zurich, Wolfgang-Pauli-Strasse 16, CH-8093 Zurich, Switzerland
[56]Max Planck Institute for Extraterrestrial Physics, Giessenbachstrasse, 85748 Garching, Germany
[57]Harvard-Smithsonian Center for Astrophysics, Cambridge, Massachusetts 02138, USA
[58]Department of Physics, University of Namibia, 340 Mandume Ndemufayo Avenue, Pionierspark, Windhoek, Namibia
[59]Lawrence Berkeley National Laboratory, 1 Cyclotron Road, Berkeley, California 94720, USA
[60]Australian Astronomical Optics, Macquarie University, North Ryde, NSW 2113, Australia
[61]Sydney Institute for Astronomy, School of Physics, A28, The University of Sydney, NSW 2006, Australia
[62]The Research School of Astronomy and Astrophysics, Australian National University, ACT 2601, Australia
[63]Department of Astronomy, The Ohio State University, Columbus, Ohio 43210, USA
[64]Department of Astrophysical Sciences, Princeton University, Peyton Hall, Princeton, New Jersey 08544, USA
[65]Institució Catalana de Recerca i Estudis Avançats, E-08010 Barcelona, Spain
[66]ARC Centre of Excellence for All-sky Astrophysics (CAASTRO), Millers Point, NSW 2000, Australia
[67]Division of Theoretical Astronomy, National Astronomical Observatory of Japan, 2-21-1 Osawa, Mitaka, Tokyo 181-8588, Japan
[68]Institute of Astronomy and Astrophysics, Academia Sinica, Taipei 10617, Taiwan
[69]Department of Physics and Astronomy, University of Waterloo, 200 University Ave W, Waterloo, Ontario N2L 3G1, Canada
[70]Perimeter Institute for Theoretical Physics, 31 Caroline St. North, Waterloo, Ontario N2L 2Y5, Canada
[71]Department of Physics and Astronomy, Pevensey Building, University of Sussex, Brighton BN1 9QH, United Kingdom
[72]ICTP South American Institute for Fundamental Research Instituto de Física Teórica, Universidade Estadual Paulista, São Paulo, Brazil
[73]Brookhaven National Laboratory, Bldg 510, Upton, New York 11973, USA
[74]Brandeis University, Physics Department, 415 South Street, Waltham, Massachusetts 02453, USA
[75]Instituto de Física Gleb Wataghin, Universidade Estadual de Campinas, 13083-859 Campinas, SP, Brazil
[76]Department of Physics, Duke University, Durham, North Carolina 27708, USA
[77]Observatories of the Carnegie Institution for Science, 813 Santa Barbara St., Pasadena, California 91101, USA
[78]Institute for Astronomy, University of Edinburgh, Edinburgh EH9 3HJ, United Kingdom

(Received 8 November 2018; revised manuscript received 19 February 2019; published 1 May 2019)

The combination of multiple observational probes has long been advocated as a powerful technique to constrain cosmological parameters, in particular dark energy. The Dark Energy Survey has measured 207 spectroscopically confirmed type Ia supernova light curves, the baryon acoustic oscillation feature, weak gravitational lensing, and galaxy clustering. Here we present combined results from these probes, deriving constraints on the equation of state, w, of dark energy and its energy density in the Universe. Independently of other experiments, such as those that measure the cosmic microwave background, the probes from this single photometric survey rule out a Universe with no dark energy, finding $w = -0.80^{+0.09}_{-0.11}$. The geometry is shown to be consistent with a spatially flat Universe, and we obtain a constraint on the baryon density of $\Omega_b = 0.069^{+0.009}_{-0.012}$ that is independent of early Universe measurements. These results demonstrate the potential power of large multiprobe photometric surveys and pave the way for order of magnitude advances in our constraints on properties of dark energy and cosmology over the next decade.

DOI: 10.1103/PhysRevLett.122.171301

Introduction.—The discovery of the accelerating Universe [1,2] revolutionized 20th century cosmology by indicating the presence of a qualitatively new component in the Universe that dominates the expansion in the last several billion years. The nature of dark energy—the component that causes the accelerated expansion—is unknown, and understanding its properties and origin is one of the principal challenges in modern physics. Current measurements are consistent with an interpretation of dark energy as a cosmological constant in general relativity. Any deviation from this interpretation in space or time would constitute a landmark discovery in fundamental physics [3].

Dark energy leaves imprints on cosmological observations, typically split into two regimes: (1) it modifies the geometry of the Universe, increasing distances and volumes in the Universe over time via the accelerated expansion, and (2) it suppresses the growth of cosmic structure. However, these effects can be mimicked by the variation of other cosmological parameters, including the dark matter density and curvature, or other physical models and systematics that are degenerate within a single probe. Consequently, measuring dark energy properties requires a combination of cosmological probes that are sensitive to both classes of effects to break these parameter and model degeneracies [4–6].

Historically, the most powerful cosmic probe has been the cosmic microwave background (CMB) [7–9], relic radiation from the surface of last scattering only 400,000 years after the big bang. Low-redshift probes measure the Universe over the last several billion years, when dark energy dominates the expansion. Comparing or combining constraints between the CMB and lower redshift measurements requires us to extrapolate predictions to the present-day Universe starting from initial conditions over 13 billion years ago. This is a powerful test of our models, but it requires precise, independent constraints from low-redshift experiments. Low-redshift probes include Type Ia supernova (SNe Ia) measurements, which treat the SNe Ia as standardizable candles and employ redshift and flux measurements to probe the redshift-luminosity distance relation [10], baryon acoustic oscillations (BAO), which use a "standard ruler" scale in the cosmic density field, imprinted by sound waves at recombination, to probe several redshift-distance combinations [11,12], galaxy clustering, which measures the density field up to some bias between galaxy density and the underlying dark matter density, and redshift-space distortions (RSD) in the clustering [13], the counts of galaxy clusters, representing the most extreme density peaks in the Universe [14], strong gravitational lensing [15], and weak gravitational lensing, which probes changes in the gravitational potential along the line of sight using coherent distortions in observed properties of galaxies or the CMB, e.g., to measure the dark and baryonic matter distribution [16].

We report here the first results from the Dark Energy Survey (DES) combining precision probes of both geometry and growth of structure that include BAO, SNe Ia, and weak lensing and galaxy clustering from a single experiment. DES has previously shown separate cosmological constraints using weak lensing and galaxy clustering [17], BAO [18], and SNe Ia [19]. We now combine these probes and begin to fully realize the power of this multiprobe experiment to produce independent measurements of the properties of dark energy.

The work presented here demonstrates our ability to extract and combine diverse cosmological observables from wide-field surveys of the evolved Universe. Previous dark energy constraints have relied on combining the likelihoods of many separate and independent experiments to produce precise constraints on cosmological models including dark energy. For this traditional approach each experiment has performed an independent analysis to validate measurements and has separate calibration methodologies and requirements, thus ensuring that many potential systematics are uncorrelated between probes. The DES analysis presented here, however, uses a common set of both calibration methodologies and systematics modeling and marginalization across probes, which enables a consistently validated analysis. Perhaps most importantly, this common framework allows us to standardize

requirements like blinding across these probes, which is essential to minimize the impact of experimenter bias [20]. This approach provides a very robust, precise cross-check of traditional multiprobe analyses, which currently provide tighter overall constraints.

The fundamental interest in understanding the nature of dark energy has spurred the development of multiple large photometric surveys that image the sky, capable of independently combining multiple cosmic probes. The current generation of surveys includes the Hyper-Suprime Cam Survey (HSC) [21], the Kilo-Degree Survey (KiDS) [22], and the focus of this work, DES [23]. The next generation of these surveys will include the Large Synoptic Survey Telescope (LSST) [24], a ground-based telescope that will observe the entire southern hemisphere with very high cadence, and space telescopes Euclid [25] and the Wide-Field InfraRed Survey Telescope (WFIRST) [26]. In parallel with imaging surveys, the distribution of galaxies measured by spectroscopic surveys (i.e., BOSS [27], eBOSS [28], and the planned 4MOST [29], DESI [30], and PFS [31] surveys) provides powerful constraints on the distance-redshift relation via BAO measurements and the growth of structure via redshift space distortions. The union of these results over the following several years, and into the next decades, will ensure that we are able to take advantage of the benefits of multiple independent, self-consistent, and blinded multiprobe analyses like we present here for DES.

Cosmic probes.—The Dark Energy Survey: DES cosmic probes span a wide range of redshifts up to $z \approx 1.3$, and include weak gravitational lensing and galaxy clustering due to large-scale structure [17], SNe Ia [19], and BAO [18]. Each probe constrains dark energy independently and their combination is more powerful. These probes utilize a subset of data from DES taken during its first three observing seasons (August 2013 to February 2016). Spectroscopically confirmed SNe Ia are identified from images in all three seasons (DES Y3) in 27 deg^2 of repeated deep-field observations, while weak lensing and large-scale structure information is derived from images taken only in the first season (DES Y1), ending February 2014 and covering 1321 deg^2 of the southern sky in *grizY* filters. DES uses the 570-megapixel Dark Energy Camera (DECam [32]) at the Cerro Tololo Inter-American Observatory (CTIO) 4m Blanco telescope in Chile. By the end of DES observations in January 2019, we anticipate an order of magnitude increase in the number of useable SNe, while the area of sky used for the other probes will increase by a factor of three to 5000 deg^2. Analysis of the later years of survey data is ongoing.

Data are processed through the DES Data Management system [33–36]. This system detrends and calibrates the raw images, creates coadded images from individual exposures, and detects and catalogs astrophysical objects. This catalog is further cleaned and calibrated to create a high-quality ("Gold") object catalog [37] from which weak lensing and large-scale structure measurements are made. The deep fields are also processed through a separate difference imaging pipeline to identify transients [38,39]. The photometric and astrometric calibrations [37] are common to all cosmology probes discussed below.

Weak gravitational lensing and large-scale structure: For weak gravitational lensing measurements, we use the measured shapes and positions of 26 million galaxies in the redshift range $0.2 < z < 1.3$, split into four redshift bins. The galaxy shapes are measured via the METACALIBRATION method [40,41] using *riz*-band exposures [42]. Photometric redshifts for the objects are determined from a modified version of the BPZ method [43], described and calibrated in Ref. [44].

For measurements of the angular galaxy clustering, we utilize the positions of a sample of luminous red galaxies that have precise photometric redshifts selected with the REDMAGIC algorithm [45]. This results in a sample of 650,000 galaxies over the redshift range $0.15 < z < 0.9$, split into five narrow redshift bins. Residual correlations of number density with survey conditions in the REDMAGIC sample are calibrated in Ref. [46]. The precise redshifts of REDMAGIC galaxies allow us to infer information about the more poorly constrained photo-z bias uncertainty in the weak lensing catalog. The photo-z calibration methodology is consistent between the weak lensing and REDMAGIC samples [44,47–49].

We use measurements from each of these galaxy samples to construct a set of three two-point correlation function observables that we label "3×2pt." These include the galaxy shear autocorrelation (cosmic shear), the galaxy position-shear crosscorrelation (galaxy-galaxy lensing), and the galaxy position autocorrelation (galaxy clustering). The analysis was described in a series of papers that include the covariance and analysis framework [50,51], the measurements and validation [46,52–54], and the cosmological results [17]. We utilize the "3×2pt" likelihood pipeline from this set of papers as implemented in COSMOSIS [55]. This combination of probes produces a tight constraint on the amplitude of matter clustering in the Universe and on the properties of dark energy over the last six billion years.

Type Ia supernovae: The DES-SN sample is comprised of 207 spectroscopically confirmed SNe Ia in the redshift range $0.07 < z < 0.85$. The sample-building and analysis pipelines are discussed in a series of papers that detail the SN Ia search and discovery [36,38,39], spectroscopic follow-up [56], photometry [57], calibration [58,59], simulations [60], and technique of accounting for selection bias [61,62]. The analysis methodology and systematic uncertainties are presented in Ref. [63]. These results are used to constrain cosmology [19] and the Hubble constant [64]. In Refs. [19,63,64] the DES-SN sample is combined with a "Low-z" ($z < 0.1$) sample, which includes SNe from the Harvard-Smithsonian Center for Astrophysics surveys

[65,66] and the Carnegie Supernova Project [67]. Selection effects and calibration of these low-redshift samples is discussed in Ref. [10]. Here we fit for DES-SN alone, and only include the Low-z sample for comparison to Ref. [19]. We compute the SNe likelihood using the SNe module [10] implemented in CosmoSIS, which is able to reproduce the results in [19].

Baryon acoustic oscillations: A sample of 1.3 million galaxies from the DES Y1 "Gold" catalog in the redshift range $0.6 < z < 1.0$ was used to measure the BAO scale in the distribution of galaxies. Details of the galaxy sample selection are in Ref. [68]. Calibrations of the galaxy selection function are consistently derived for the BAO and "3×2pt" samples. This BAO measurement was presented in Ref. [18] and provides a likelihood for the ratio between the angular diameter distance to redshift 0.81, $D_A(z = 0.81)$, and the sound horizon at the drag epoch, r_d. This analysis used 1800 simulations [69] and three methods to compute the galaxy clustering [70–72]. The BAO likelihood is implemented in CosmoSIS. The galaxy samples used in the "3×2pt" angular clustering measurements and in the BAO analysis share a common footprint in the sky and overlap significantly in volume over the redshift range $0.6 < z < 0.9$, which will produce some nonzero correlation between the two measurements. However, the intersection of the galaxy populations is only about 14% of the total BAO galaxy sample and we detect no significant BAO constraint when using the "3x2pt" galaxy clustering measurements. We thus ignore this negligible correlation when combining the two probes.

External data for comparison: We use external constraints that combine state-of-the-art CMB, SNe Ia, and spectroscopic BAO measurements to compare our results against. For the CMB data, we utilize full-sky temperature (T) and polarization (E- and B-mode) measurements from the Planck survey, combining TT ($\ell \in [2, 2508]$), and EE, BB and TE ($\ell \in [2, 29]$) (commonly referred to as "TT + LowP") [73] with weak lensing measurements derived from the temperature data [74]. We use the Planck likelihood from Ref. [75].

For external SNe Ia measurements, we use the Pantheon compilation [10]. Pantheon combines SNe Ia samples from Pan-STARRS1, SDSS, SNLS, various low-z data sets, and HST. The Pantheon data set is based on the Pan-STARRS1 Supercal algorithm [76] that establishes a global calibration for the 13 different SNe Ia samples, with a total of 1048 SNe in $0.01 < z < 2.26$.

Finally, external spectroscopic BAO measurements are taken from BOSS DR12 [13], the 6dF Galaxy Survey [77], and the SDSS Main Galaxy Sample [78]. These measurements of the BAO scale span a redshift range of $0.1 < z < 0.6$.

Constraints on dark energy.—We present here a dark energy analysis that combines for the first time the DES probes described above. DES is able to strongly constrain dark energy models without the CMB by probing over a wide redshift range ($z \lesssim 1$) the growth of structure and distance-redshift relation, which are both sensitive to the presence of dark energy. The dark energy equation of state w relates the pressure (P) to the energy density (ρ) of the dark energy fluid: $w = P/\rho$, where $w = -1$ is equivalent to a cosmological constant Λ in the field equations. We probe the nature of dark energy in two ways: (1) we constrain the dark energy density relative to the critical density today, Ω_Λ, assuming that dark energy takes the form of a cosmological constant and allowing nonzero curvature (the oCDM model), and (2) we measure w as a free parameter (the wCDM model) with fixed curvature ($\Omega_k = 0$). The total energy density of the Universe today is composed of the sum of fractional components $1 = \Omega_k + \Omega_m + \Omega_\Lambda$, where the components are: curvature (Ω_k), the total matter (Ω_m), and dark energy (Ω_Λ). The radiation density is assumed to be negligible over the redshift ranges probed by DES.

In both oCDM and wCDM models, we explore the ability of DES to constrain these properties of dark energy and compare this to the state-of-the-art constraints combining measurements from many external surveys. We follow the analysis methods and model definitions from Ref. [17], which includes varying the neutrino mass density in all models. External data are re-analyzed to make direct comparisons meaningful, including matching parameter choices and priors to the DES analysis. The cosmological parameters and their priors are slightly changed from Ref. [17] and listed in Table I. Noncosmological parameters and their priors are identical to Table I of Ref. [17], with the absolute magnitude $-19.5 < \mathcal{M} < -18.9$ for SNe. Cosmological parameters and the intrinsic alignment model (for "3×2pt") are shared between probes. The joint posterior is the product of the individual posteriors of the three probes, which are assumed to be sufficiently

TABLE I. Cosmological parameter constraints in the oCDM and wCDM models using only DES data. We report the 1D peak of the posterior and asymmetric 68% confidence limits. The marginalized parameters with informative priors (and prior ranges) are: the primordial perturbation amplitude $10^9 A_s \in [0.5, 10.0]$, the Hubble constant $H_0 \in [55, 90]$ km s^{-1} Mpc^{-1}, the spectral index $n_s \in [0.87, 1.07]$, and the neutrino mass density $\Omega_\nu h^2 \in [0.0006, 0.01]$.

Parameter	oCDM	wCDM	wCDM (Ext)	Flat prior
Ω_m	$0.299^{+0.024}_{-0.020}$	$0.300^{+0.023}_{-0.021}$	$0.303^{+0.007}_{-0.009}$	[0.1, 0.9]
Ω_b	$0.069^{+0.009}_{-0.012}$	$0.064^{+0.013}_{-0.009}$	$0.048^{+0.001}_{-0.001}$	[0.03, 0.12]
Ω_k	$0.252^{+0.095}_{-0.14}$	0	0	[-0.1, 0.5]
Ω_Λ	$0.47^{+0.14}_{-0.12}$	$0.700^{+0.021}_{-0.023}$	$0.697^{+0.009}_{-0.007}$	Derived
w	-1	$-0.80^{+0.09}_{-0.11}$	$-1.02^{+0.03}_{-0.04}$	[-2, -0.33]
S_8	$0.801^{+0.028}_{-0.026}$	$0.786^{+0.029}_{-0.019}$	$0.814^{+0.016}_{-0.011}$	Derived

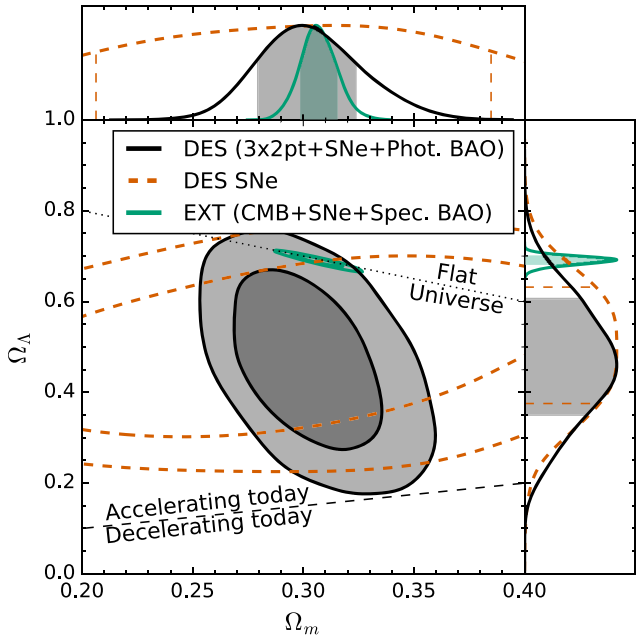

FIG. 1. Constraints on the present-day dark energy density Ω_Λ and matter density Ω_m, relative to the critical density, in an oCDM model with marginalized curvature and neutrino mass density. We compare the constraint from DES data alone (black contours), including information from weak gravitational lensing, large-scale structure, SNe Ia, and photometric BAO, to the best available external data (green contours), combining information from the CMB, SNe Ia, and spectroscopic BAO. We identify the flat model ($\Omega_k = 0$) with a dotted line and distinguish accelerating and decelerating universes with a dashed line. Contours represent the 68% and 95% confidence limits (CL).

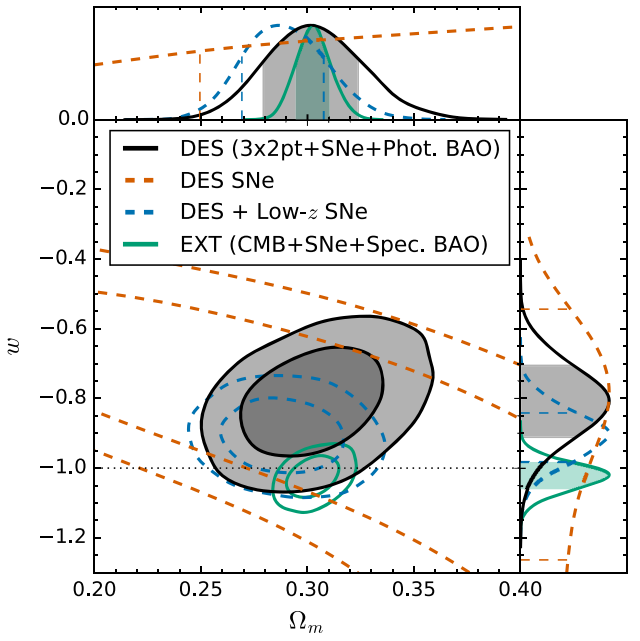

FIG. 2. Constraints on the dark energy equation of state w and Ω_m in a wCDM model with fixed curvature ($\Omega_k = 0$) and marginalized neutrino mass density. We compare constraints from the DES data alone (black contours) to the best available external data (green contours), as in Fig. 1, but also show the impact of including a low-redshift SNe Ia data set (Low-z) to anchor the DES SNe Ia as done in Ref. [19] (blue contours). Each component of the DES analysis was fully blinded.

independent at this precision, as motivated in the previous section.

Figure 1 shows our constraints on Ω_Λ in the oCDM model, where $w = -1$. We combine our "3×2pt," SNe Ia (without the external Low-z sample), and photometric BAO measurements to constrain Ω_Λ and Ω_m. This is compared to the constraint from the external data sets. The DES best-fit χ^2 is 576 with 498 degrees of freedom (dof) [79]. Using DES data we are able to independently confirm the existence of a dark energy component in the Universe ($\Omega_\Lambda > 0$) at $\sim 4\sigma$ significance. This is the first time a photometric survey has independently made a significant constraint on the energy density of both dark energy and dark matter without assuming a flat model based on early Universe constraints. It represents an important milestone for future analyses from DES and surveys like Euclid, LSST, and WFIRST.

In Fig. 2, we show the constraint on w and Ω_m, assuming the wCDM model. We show the same comparison with external data as in Fig. 1, but also include a case where we supplement DES-discovered SNe Ia with the Low-z SNe sample to anchor the SNe redshift-distance relation at low redshift following Ref. [19]. This low-redshift SNe anchor contributes significantly to both the DES + Low-z and external constraints on w. In all cases, the existing data are consistent with a cosmological constant ($w = -1$). The DES best-fit χ^2 is 577 with 498 dof. This subset of the final DES data constrains w to within a factor of three of the combined external constraint. This result illustrates the prospects for multiple independent, precise low-redshift constraints on dark energy from upcoming large-scale photometric experiments.

The constraints on all cosmological model parameters are summarized in Table I. Nuisance parameter constraints are not qualitatively changed from individual probe fits. The DES-only "3×2pt" and SNe data are consistent and individually contribute similar constraining power for w and Ω_Λ. In the oCDM model, DES constrains the total matter density to 7% (68% CL), the baryon density to 15%, and the correlation amplitude to 3%, described by $S_8 \equiv \sigma_8 \sqrt{\Omega_m/0.3}$, where σ_8 measures the current-day clustering amplitude. The constraints are comparable in wCDM. Fixing $\Omega_k = 0$, we find the S_8 constraint is improved by a factor of 1.2, but there is otherwise no significant improvement in other parameters. The parameter constraints beyond dark energy are driven by the "3×2pt" measurement. In particular, the baryon density constraint is due to sensitivity to the shape of the matter power spectrum from baryon damping [80]. The constraint on Ω_b from the CMB, by contrast, is also sensitive to the

impact of baryons on the acoustic oscillations. Thus future low-redshift survey data will provide another avenue to test the predictions of our models from early Universe observations like the CMB with measurements of Ω_b from surveys like DES.

Outlook.—The most precise constraints on dark energy properties require combining cosmological probes that include information from both geometry and growth across cosmic history. Thus far such diverse information was collected from different experiments, which were subject to different calibration and systematic errors. We have combined for the first time in DES the purely cosmographic SN and BAO measurements with the growth-sensitive weak lensing and galaxy clustering measurements to independently place strong constraints on the nature of dark energy. These results share a common set of calibration frameworks and blinding policy across probes. DES has independently constrained Ω_m, Ω_b, Ω_Λ, σ_8, and w, while marginalizing over a free neutrino mass. We expect future DES results to provide a further factor of 2–4 improvement in these constraints due to increased area, depth, and number of SNe in the final analyses, which will then be followed by subsequent order of magnitude advances from more sensitive photometric surveys of the 2020s.

Funding for the DES Projects has been provided by the DOE and NSF (USA), MEC/MICINN/MINECO (Spain), STFC (UK), HEFCE (United Kingdom), NCSA (UIUC), KICP (U. Chicago), CCAPP (Ohio State), MIFPA (Texas A&M), CNPQ, FAPERJ, FINEP (Brazil), DFG (Germany), and the Collaborating Institutions in the Dark Energy Survey. The Collaborating Institutions are Argonne Lab, UC Santa Cruz, University of Cambridge, CIEMAT-Madrid, University of Chicago, University College London, DES-Brazil Consortium, University of Edinburgh, ETH Zürich, Fermilab, University of Illinois, ICE (IEEC-CSIC), IFAE Barcelona, Lawrence Berkeley Lab, LMU München and the associated Excellence Cluster Universe, University of Michigan, NOAO, University of Nottingham, Ohio State University, University of Pennsylvania, University of Portsmouth, SLAC National Lab, Stanford University, University of Sussex, Texas A&M University, and the OzDES Membership Consortium. Based in part on observations at Cerro Tololo Inter-American Observatory, National Optical Astronomy Observatory, which is operated by the Association of Universities for Research in Astronomy (AURA) under a cooperative agreement with the National Science Foundation. The DES Data Management System is supported by the NSF under Grants No. AST-1138766 and No. AST-1536171. The DES participants from Spanish institutions are partially supported by MINECO under Grants No. AYA2015-71825, No. ESP2015-66861, No. FPA2015-68048, No. SEV-2016-0588, No. SEV-2016-0597, and No. MDM-2015-0509, some of which include ERDF funds from the European Union. IFAE is partially funded by the CERCA program of the Generalitat de Catalunya. Research leading to these results has received funding from the European Research Council under the European Union's Seventh Framework Program (FP7/2007-2013) including ERC Grants No. 240672, No. 291329, and No. 306478. We acknowledge support from the Australian Research Council Centre of Excellence for All-sky Astrophysics (CAASTRO), through Project No. CE110001020, and the Brazilian Instituto Nacional de Ciência e Tecnologia (INCT) e-Universe (CNPq Grant No. 465376/2014-2). This Letter has been authored by Fermi Research Alliance, LLC under Contract No. DE-AC02-07CH11359 with the U.S. Department of Energy, Office of Science, Office of High Energy Physics. The United States Government retains and the publisher, by accepting the article for publication, acknowledges that the United States Government retains a nonexclusive, paid-up, irrevocable, world-wide license to publish or reproduce the published form of this manuscript, or allow others to do so, for United States Government purposes. This research used resources of the National Energy Research Scientific Computing Center, a DOE Office of Science User Facility supported by the Office of Science of the U.S. Department of Energy under Contract No. DE-AC02-05CH11231. This Letter also used resources on the CCAPP condo of the Ruby Cluster at the Ohio Supercomputing Center [81]. Plots in this Letter were produced partly with MATPLOTLIB [82], and it has been prepared using NASA's Astrophysics Data System Bibliographic Services.

[1] A. G. Riess *et al.* (Supernova Search Team), Astron. J. **116**, 1009 (1998).
[2] S. Perlmutter *et al.* (Supernova Cosmology Project), Astrophys. J. **517**, 565 (1999).
[3] A. Albrecht *et al.*, arXiv:astro-ph/0609591.
[4] J. Frieman, M. Turner, and D. Huterer, Annu. Rev. Astron. Astrophys. **46**, 385 (2008).
[5] D. H. Weinberg, M. J. Mortonson, D. J. Eisenstein, C. Hirata, A. G. Riess, and E. Rozo, Phys. Rep. **530**, 87 (2013).
[6] D. Huterer and D. L. Shafer, Rep. Prog. Phys. **81**, 016901 (2018).
[7] W. Hu and S. Dodelson, Annu. Rev. Astron. Astrophys. **40**, 171 (2002).
[8] G. Hinshaw *et al.*, Astrophys. J. Suppl. Ser. **208**, 19 (2013).
[9] N. Aghanim *et al.* (Planck Collaboration), arXiv:1807.06209.
[10] D. M. Scolnic *et al.*, Astrophys. J. **859**, 101 (2018).
[11] L. Anderson *et al.*, Mon. Not. R. Astron. Soc. **441**, 24 (2014).
[12] J. E. Bautista *et al.*, Astrophys. J. **863**, 110 (2018).
[13] S. Alam *et al.*, Mon. Not. R. Astron. Soc. **470**, 2617 (2017).
[14] S. W. Allen, A. E. Evrard, and A. B. Mantz, Annu. Rev. Astron. Astrophys. **49**, 409 (2011).
[15] S. H. Suyu *et al.*, Mon. Not. R. Astron. Soc. **468**, 2590 (2017).

[16] R. Mandelbaum, Annu. Rev. Astron. Astrophys. **56**, 393 (2018).
[17] T. M. C. Abbott *et al.* (DES Collaboration), Phys. Rev. D **98**, 043526 (2018).
[18] T. M. C. Abbott *et al.* (DES Collaboration), arXiv: 1712.06209.
[19] T. M. C. Abbott *et al.* (DES Collaboration), Astrophys. J. Lett. **872**, L30 (2019).
[20] R. A. C. Croft and M. Dailey, Q. Phys. Rev. **2015**, 1 (2015).
[21] http://hsc.mtk.nao.ac.jp/ssp/.
[22] http://kids.strw.leidenuniv.nl.
[23] http://www.darkenergysurvey.org/.
[24] http://www.lsst.org.
[25] http://sci.esa.int/euclid.
[26] http://wfirst.gsfc.nasa.gov.
[27] http://www.sdss3.org/surveys/boss.php.
[28] https://www.sdss.org/surveys/eboss.
[29] https://www.4most.eu/cms.
[30] https://www.desi.lbl.gov/.
[31] https://pfs.ipmu.jp.
[32] B. Flaugher *et al.* (DES Collaboration), Astron. J. **150**, 150 (2015).
[33] S. Desai *et al.*, Astrophys. J. **757**, 83 (2012).
[34] I. Sevilla *et al.* (DES Collaboration), arXiv:1109.6741.
[35] J. J. Mohr *et al.*, in Proc. SPIE Int. Soc. Opt. Eng. **7016**, 70160L (2008).
[36] E. Morganson *et al.* (DES Collaboration), Publ. Astron. Soc. Pac. **130**, 074501 (2018).
[37] A. Drlica-Wagner *et al.* (DES Collaboration), Astrophys. J. Suppl. Ser. **235**, 33 (2018).
[38] D. A. Goldstein *et al.* (DES Collaboration), Astron. J. **150**, 82 (2015).
[39] R. Kessler *et al.* (DES Collaboration), Astron. J. **150**, 172 (2015).
[40] E. Huff and R. Mandelbaum, arXiv:1702.02600.
[41] E. S. Sheldon and E. M. Huff, Astrophys. J. **841**, 24 (2017).
[42] J. Zuntz *et al.* (DES Collaboration), Mon. Not. R. Astron. Soc. **481**, 1149 (2018).
[43] N. Benítez, Astrophys. J. **536**, 571 (2000).
[44] B. Hoyle *et al.* (DES Collaboration), Mon. Not. R. Astron. Soc. **478**, 592 (2018).
[45] E. Rozo *et al.* (DES Collaboration), Mon. Not. R. Astron. Soc. **461**, 1431 (2016).
[46] J. Elvin-Poole *et al.* (DES Collaboration), Phys. Rev. D **98**, 042006 (2018).
[47] R. Cawthon *et al.* (DES Collaboration), Mon. Not. R. Astron. Soc. **481**, 2427 (2018).
[48] M. Gatti *et al.* (DES Collaboration), Mon. Not. R. Astron. Soc. **477**, 1664 (2018).
[49] C. Davis *et al.* (DES Collaboration), arXiv:1710.02517.
[50] E. Krause and T. Eifler, Mon. Not. R. Astron. Soc. **470**, 2100 (2017).
[51] E. Krause *et al.* (DES Collaboration), arXiv:1706.09359.
[52] N. MacCrann *et al.* (DES Collaboration), Mon. Not. R. Astron. Soc. **480**, 4614 (2018).
[53] J. Prat *et al.* (DES Collaboration), Phys. Rev. D **98**, 042005 (2018).
[54] M. A. Troxel *et al.* (DES Collaboration), Phys. Rev. D **98**, 043528 (2018).
[55] J. Zuntz *et al.*, Astron. Comput. **12**, 45 (2015).
[56] C. D'Andrea *et al.* (DES Collaboration) (to be published).
[57] D. Brout *et al.*, arXiv:1811.02378.
[58] D. L. Burke *et al.*, Astron. J. **155**, 41 (2018).
[59] J. Lasker *et al.*, arXiv:1811.02380.
[60] R. Kessler *et al.*, Mon. Not. R. Astron. Soc. **485**, 1171 (2019).
[61] R. Kessler and D. Scolnic, Astrophys. J. **836**, 56 (2017).
[62] D. Scolnic and R. Kessler, Astrophys. J. Lett. **822**, L35 (2016).
[63] D. Brout *et al.*, arXiv:1811.02377.
[64] E. Macauley *et al.*, arXiv:1811.02376.
[65] M. Hicken, W. M. Wood-Vasey, S. Blondin, P. Challis, S. Jha, P. L. Kelly, A. Rest, and R. P. Kirshner, Astrophys. J. **700**, 1097 (2009).
[66] M. Hicken *et al.*, Astrophys. J. Suppl. Ser. **200**, 12 (2012).
[67] C. Contreras *et al.*, Astron. J. **139**, 519 (2010).
[68] M. Crocce *et al.* (DES Collaboration), Mon. Not. R. Astron. Soc. **482**, 2411 (2018).
[69] S. Avila *et al.* (DES Collaboration), Mon. Not. R. Astron. Soc. **479**, 94 (2018).
[70] A. J. Ross *et al.* (DES Collaboration), Mon. Not. R. Astron. Soc. **472**, 4456 (2017).
[71] K. C. Chan *et al.* (DES Collaboration), Mon. Not. R. Astron. Soc. **480**, 3031 (2018).
[72] H. Camacho *et al.* (DES Collaboration), arXiv:1807.10163.
[73] P. A. R. Ade *et al.* (Planck Collaboration), Astron. Astrophys. **594**, A13 (2016).
[74] P. A. R. Ade *et al.* (Planck Collaboration), Astron. Astrophys. **594**, A15 (2016).
[75] N. Aghanim *et al.* (Planck Collaboration), Astron. Astrophys. **594**, A11 (2016).
[76] D. Scolnic *et al.*, Astrophys. J. **815**, 117 (2015).
[77] F. Beutler, C. Blake, M. Colless, D. Heath Jones, L. Staveley-Smith, L. Campbell, Q. Parker, W. Saunders, and F. Watson, Mon. Not. R. Astron. Soc. **416**, 3017 (2011).
[78] A. J. Ross, L. Samushia, C. Howlett, W. J. Percival, A. Burden, and M. Manera, Mon. Not. R. Astron. Soc. **449**, 835 (2015).
[79] For further discussion of the χ^2 value, see Ref. [83] (Section IV on Light curve fitting and bias corrections).
[80] This constraint on Ω_b is not prior driven, despite being degenerate with A_s and n_s (which is unconstrained).
[81] OSC, "Ohio supercomputer center," http://osc.edu/ark:/19495/f5s1ph73.
[82] J. D. Hunter, Comput. Sci. Eng. **9**, 90 (2007).
[83] https://des.ncsa.illinois.edu/releases/sn.